Thermal Efficiency for Hydronic Bridge-Road Heating

H. TERASAKI, A. SAIDA & T. FUKUHARA
Department of Architecture and Civil Engineering, University of Fukui, Japan
TERASAKI@U-FUKUI.AC.JP
A. FUJIMOTO
Traffic Engineering Research Team, Civil Engineering Research Institute for Cold Region, Japan
afujimot@ceri.go.jp

ABSTRACT

Thermal efficiency is one of the most important design parameters for a hydronic bridge-road heating system. In this system, heat is transferred in a small-diameter channel of circular shape as a heat-carrier fluid passage under the bridge pavement. The heat flow at the road surface $\overline{q_{pav}}$ is dissipated to melt snow on the road surface. The thermal efficiency η is defined as the ratio of $\overline{q_{pav}}$ to heat flow $\overline{q_{sup}}$ that is supplied to the pavement from fluid in the heat-carrier passage. To understand the properties of η, a heat transfer model of a hydronic bridge-road heating (HBRH model) was constructed. The reliability of the HBRH model was confirmed by comparing the model predictions with experimentally observed temperature profiles in the hydronically-heated bridge road, which consists of a surface course, a base course containing the heat-carrier fluid passages, and a concrete slab.

The results show that η diminishes with the increasing thickness of the surface course, thermal conductivity of the deck slab, and overburden depth of the heat-carrier fluid passage, and grows with the increasing thermal conductivity of the surface course and base course.

1. INTRODUCTION

Bridges are particularly vulnerable to icing[1), 2)] because bridge road surfaces receive no heat from underlying ground and have low heat capacity. Bridges, therefore, increase the need for frequent applications of anti-freezing agents, which, in turn, increase the labor and economic expense.

Due to all of the above concerns, it is common to mount road heating systems on bridges and viaducts[3)–5)]. In a hydronic bridge-road heating system, a heat-carrier fluid, which is warmed by natural heat sources such as the ground, a lake, a river, etc., circulates through heat exchanger piping (heating coils) installed in the pavement to provide heat to warm the pavement, and then returns to the heat sources to be re-warmed.

The design standards for melting snow on road surfaces[6)] in the Hokuriku and North Kinki regions have usually been followed in the guideline of hydronic bridge-road heating systems created by the Hokuriku Bureau of the Ministry of Land, Infrastructure, Transport and Tourism. The design heat for melting snow or for preventing icing is calculated by dividing the heat for melting snow or for preventing icing by the thermal efficiency, η. Specifically, η is the ratio of the heat flow at the road surface $\overline{q_{pav}}$ to the heat flow supplied from the heat-carrier fluid $\overline{q_{sup}}$ (i.e. $\overline{q_{pav}}/\overline{q_{sup}}$; see Figure 1). η may be affected by internal parameters including the thermal properties and thickness of the roadway and the depth of

a heat exchange piping or a heat-carrier fluid passage below the road surface (overburden depth), and by external parameters including the micrometeorology at the upper and lower bridge surfaces. The design standards of the facilities for melting snow on road surfaces specify some values, e.g. η = 0.65 for concrete deck slabs, although no unequivocal physical basis is known for such parameters. We created, therefore, a heat transfer analysis model of what is called here a “hydronic bridge-road heating” (HBRH) model.

The purpose of this study is to identify the influence of both internal road parameters and external conditions on η by using the HBRH model and laboratory experimental results.

2. HEAT TRANSFER THEORY

2.1. Overview of the HBRH model

As shown in Figure 1, the hydronically-heated bridge road (HHBR) consists of three layers: a surface course, a base course containing heat-carrier fluid passages, and a concrete deck slab (hereinafter, “deck slab”). The following assumptions were made in this analysis:

(1) η is applied to heat transfer in the transversal direction (x) and the vertical direction (z), but heat transfer in the direction of the heat-carrier fluid passage (y) is neglected.
(2) Vehicle-related heat fluxes, precipitation or phase changes are neglected.

The analytical domain is within the dashed lines (abb'a') in Figure 1. The boundary conditions at the upper border of the analytical domain (the road surface) and the lower border (the bottom surface of the deck slab) are also illustrated in Figure 1. Borders a-a' and b-b' are assumed to have no heat transfer on the basis of symmetry of the temperature profile with respect to the z-axis (a-a' or b-b').

2.2. Fundamental equations

Heat transfer in the surface course, base course, and deck slab (*sc*, *bc*, and *ds*, respectively) is described by the following two-dimensional heat conduction equation:

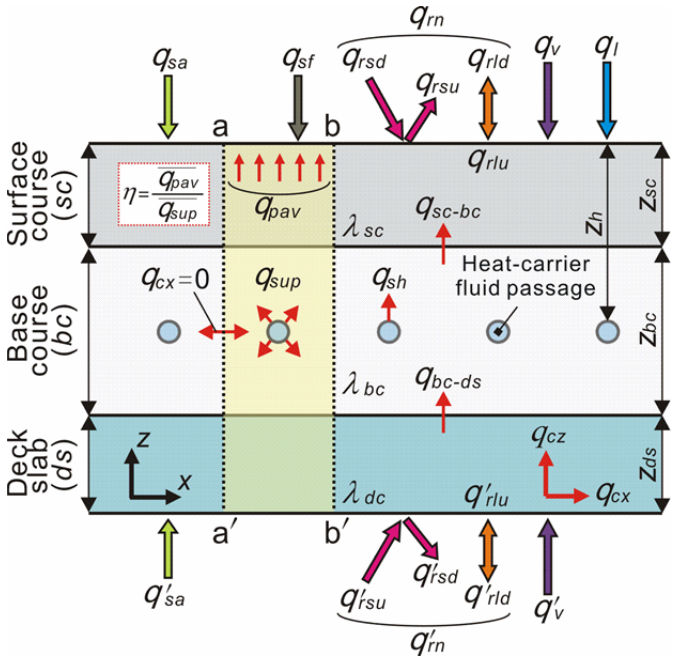

Figure 1 - Heat fluxes in the hydronic bridge-road heating (HBRH) model

$$(\rho c)\frac{\partial T}{\partial t} = -\frac{\partial q_{cx}}{\partial x} - \frac{\partial q_{cz}}{\partial z} + q_{sup}\xi\,, \tag{1}$$

where T is the temperature, ρc (J/m^{3}K) is the volumetric heat capacity, and t is the time (s). q_{sup} (W/m^2) is the heat flux supplied from the heat-carrier fluid, which is added only to elements neighboring the heat-carrier fluid passages (adjacent elements). ξ (1/m) is the ratio of the contact area of the heat-carrier fluid passage to the volume of the adjacent element. In accordance with Newton's law of cooling, q_{sup} is found as follows:

$$q_{sup} = \alpha_{sh}(T_w - T), \tag{2}$$

where α_{sh} (W/m^{2}K) is the heat transfer coefficient between the heat-carrier fluid and the base course, T_w is the temperature of the heat-carrier fluid (ºC).

q_{cx} and q_{cz} (W/m^2) are the conductive heat flux in the x and z directions, respectively, and are calculated by Fourier's law:

$$q_{cx} = -\lambda\frac{\partial T}{\partial x},\ q_{cz} = -\lambda\frac{\partial T}{\partial z}, \tag{3}$$

where λ (W/mK) is the thermal conductivity. q_{cz} at the interface between the layers making up the HHBR is calculated in the next equation using the contact thermal resistance r (m^{2}K/W). For example, q_{cz} at the interface between the surface course and the base course is calculated as follows:

$$q_{cz} = \frac{1}{\frac{\Delta z_{sc}}{\lambda_{sc}} + \frac{\Delta z_{bc}}{\lambda_{bc}} + r_{sc-bc}}(T_{scb} - T_{bct}), \tag{4}$$

Here, $r_{sc\text{-}bc}$ is the contact thermal resistance between the surface course and the base course, T_{scb} is the temperature of the surface course element where it contacts the base course, T_{bct} is the temperature of the base course element where it contacts the surface course. The above analogy is adapted to q_{cz} at the interface between the base course and the deck slab.

The sensible heat due to wind and net radiant heat are taken into consideration in the heat balance at the road surface or the bottom surface of deck slab.

3. VERIFICATION OF THE HBRH MODEL

3.1. Overview of laboratory heat transfer experiment

Figure 2 is a diagram of the HHBR specimen and the experiment was carried out in a temperature controlled room.

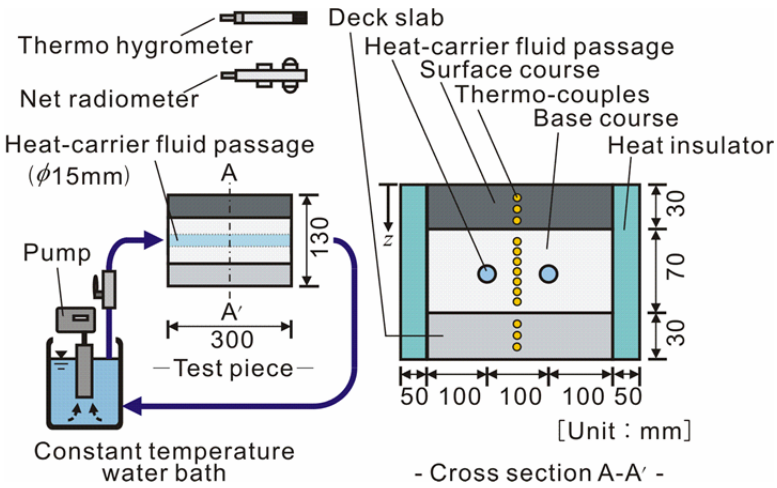

Figure 2 - Diagram of laboratory heat transfer experiment using hydronically-heated bridge road

Figure 3 shows vertical cross sections of the five specimens, designated specimen A through specimen E. The surface course (30 mm thick) was a porous asphalt mixture, the base course (70 mm thick) was silica concrete, ordinary concrete, or mastic, and the deck slab (30 mm thick) was silica concrete or ordinary concrete. To suppress the vertical heat conduction to the deck slab in specimen E, a heat insulator (30 mm thick) was placed between the base course and the deck slab. The heat-carrier fluid passages were 15 mm in diameter at a 100 mm pitch. The overburden depth of the heat-carrier fluid passages was 47.5 mm in specimen B and 82.5 mm in all the other specimens. In specimen D, steel tubes with I.D. 15 mm and O.D. 17 mm were used in place of the heat-carrier fluid passages. The upper and lower surfaces of the specimen stayed in contact with the air. The sides of the specimens were covered with a 50 mm thick heat insulator. Thirteen thermocouples were placed between the heat-carrier fluid passages in the plane defined by their centerlines.

The experimental procedure was as follows: (i) The specimen was allowed to settle in the ambient air to establish the initial uniform temperature, (ii) The heat-carrier fluid was circulated through the heat-carrier fluid passages and a thermostatically controlled bath, (iii) Once the specimen temperature reached steady state, the experiment was concluded.

The experimental conditions were as follows: ambient air temperature 5 ºC, heat-carrier fluid circulating temperature 40 ºC, and flow rate 0.6 l/min.

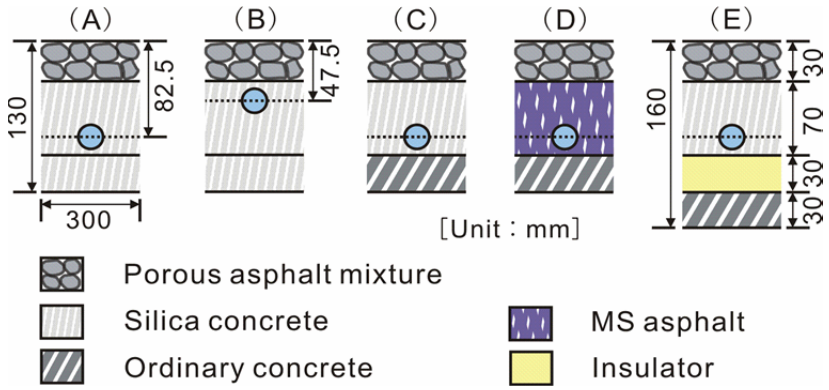

Figure 3 - Cross sections of specimens for hydronically-heated bridge road

3.2. Analytical conditions

Table 1 provides the thermal properties and parameters of the specimens used in this experiment. The thermal resistance r and the heat transfer coefficient α_{sh} were set to match the calculated results of the vertical temperature distribution in the specimens with the measured results. The thermo-physical values not published in the references were found in this experiment.

3.3. Comparison of experimental findings with calculated values

Figure 4 shows the time variations in the vertical distribution of specimen temperature $T(z)$ over the experiment duration of 13 hours. z=0 is the road surface. The symbols and lines in the figure represent experimental and calculated values, respectively.

Table 1 - Thermal properties and parameters of the specimens

Prameters		Unit	Porous asphalt mixture	Silica concrete	Ordinary concrete	Mastic asphlt	Heat insulator
Heat capacity	(ρc)	kJ/m^{3}K	1600	2090	1900	1600	54.3[8]
Thermal conductivity	λ	W/mK	0.90[7]	2.20[9]	1.59[9]	1.42	0.04[8]
Heat transfer coefficient between heat-carrier fluid and concrete	α_{sh}	W/m^{2}K	—	350	—	80	—
Heat transfer coefficient between air and surface	α_{sa}	W/m^{2}K	2.2[10]	2.2[10]	2.2[10]	—	—
Emmisivity	ε	—	0.95	0.94[8]	0.95[8]	—	—

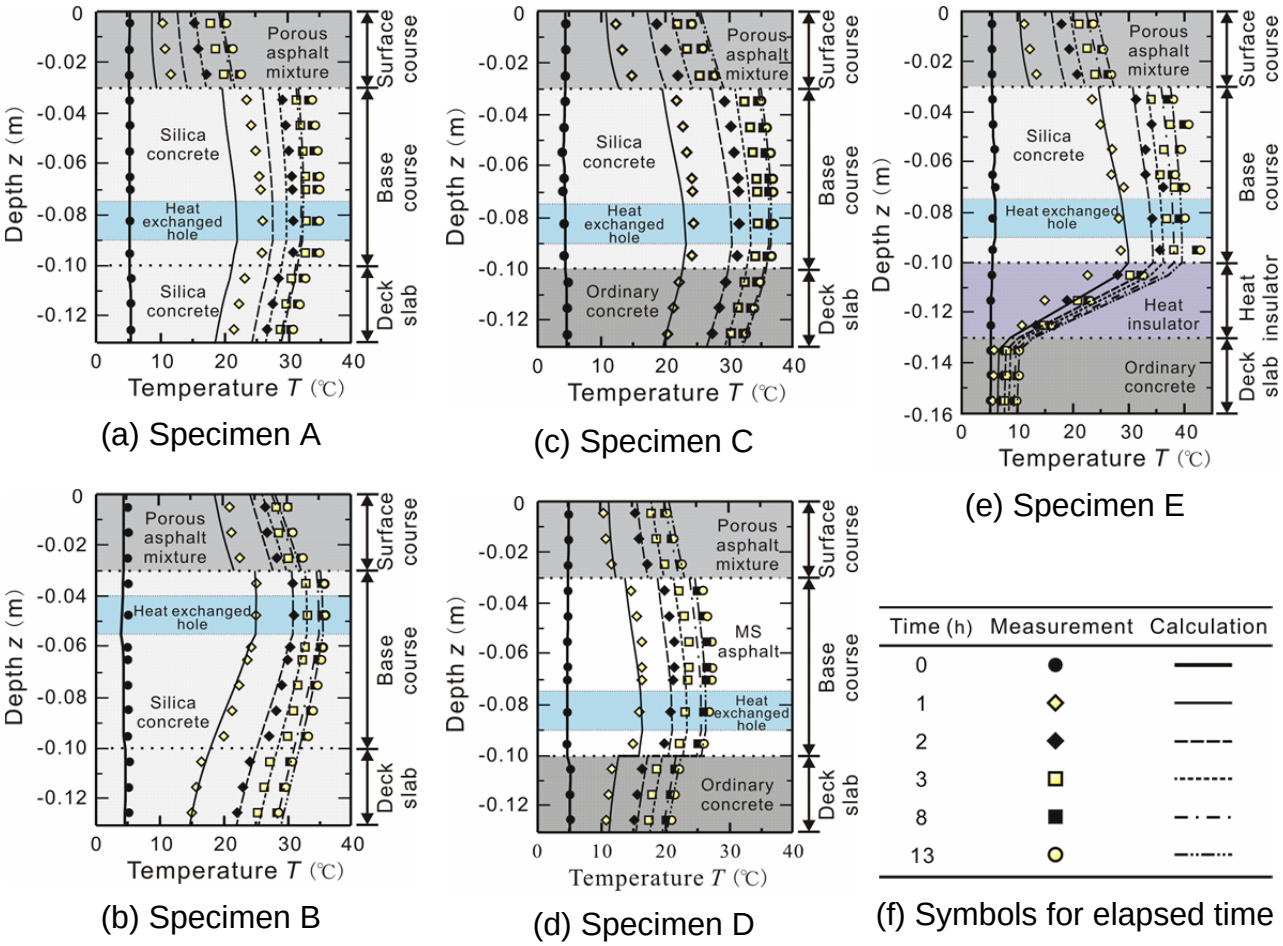

Figure 4 - Time variations in the vertical distribution of temperatures in specimens

The calculated vertical distributions of T_{sc}, T_{bc}, and T_{ds} matched well with the measured values, and thus demonstrated the validity of the HBRH model. In specimen A, the measured T_{sc} and T_{bc} were approximately 3 ºC lower than the calculated values during t = 1 to 3 h (after initiation of the experiment). This may be attributed to discrepancies in the thermal properties of the specimen used in the calculations.

Finally, η was calculated by integration of the conductive heat flux at the road surface in a thermal equilibrium (t = 13 h) by the following equation:

$$\eta = \frac{\overline{q_{pav}}}{\overline{q_{sup}}} = \frac{\int_a^b q_{cz|z=0} dx}{\int_{S^t} q_{sup} ds}, \tag{5}$$

where $\overline{q_{pav}}$ is the conductive heat flow at the road surface (road-surface heat flux). The interval between a-a' and b-b' was the size of the analytical domain in the x direction (see Figure 1). S^t is the circumference of the heat-carrier fluid passage and ds is a small portion of the circumference. The values of η for specimens A through E were 0.26, 0.39, 0.32, 0.32, and 0.65, respectively, and revealed that η varied with the thicknesses and thermal properties of the paving and deck slab and with the overburden depth of the heat-carrier fluid passage.

4. CHARACTERISTICS OF THERMAL EFFICIENCY

The above findings allowed us to identify the influence of internal parameters such as the pavement structure and thermal properties on η by using a sensitivity analysis under steady-state meteorological conditions.

Variables in this sensitivity analysis were the layer thicknesses of the HHBR (z_{sc} and z_{ds}), thermal conductivities (λ_{sc}, λ_{bc}, and λ_{ds}), and the overburden depth of the heat-carrier fluid passages (z_h). To simplify the characteristics of η, each variable was written in the following dimensionless form:

$$P^* = \frac{P}{P_0}, \tag{6}$$

where P is any of z_{sc}, z_{ds}, λ_{sc}, λ_{bc}, λ_{ds}, or z_h, and P_0 is a representative value of each P.

Figure 5(a) shows all of the variables used in the sensitivity analysis. For the representative value of P_0, η was 0.59.

Figure 5(b) through (f) show how η varied with P^*. We can see that η diminished exponentially with the increase in the parameters z_{sc}^*, λ_{ds}^*, and z_h^*, but increased logarithmically with the increase in λ_{sc}^* and λ_{bc}^*. From Figure 5, it was found that the order of these parameters in terms of sensitivity to η was from highest to lowest, λ_{ds}^*, z_{sc}^*, λ_{sc}^*, z_h^*, and λ_{bc}^*.

	P_0	P	Unit
z_{sc}	50	25～150	mm
z_{ds}	300	150～	mm
λ_{sc}	0.9	0.5～2.7	W/mK
λ_{bc}	2.2	1.3～6.9	W/mK
λ_{ds}	1.6	0.8～4.8	W/mK
z_h	70	35～210	mm

(a) Variables used in sensitivity analysis

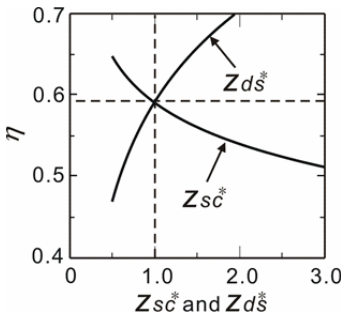

(b) z_{sc}^* and z_{ds}^*

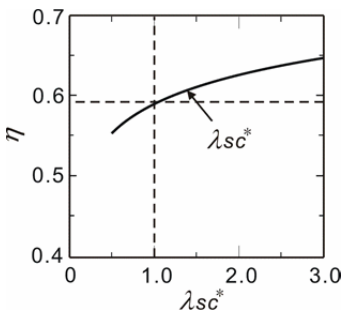

(c) λ_{sc}^*

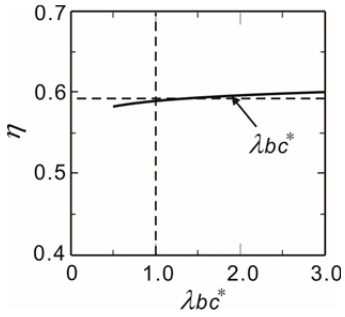

(d) λ_{bc}^*

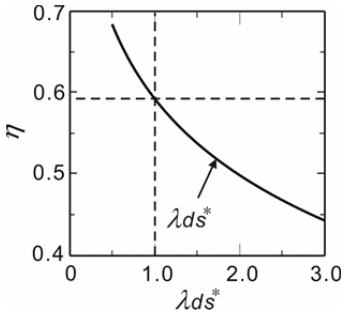

(e) λ_{ds}^*

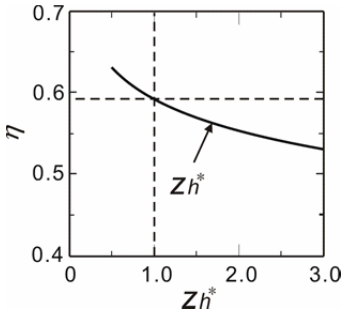

(f) z_h^*

Figure 5 - Influence of layer thickness, thermal conductivity, and heat-carrier fluid passage cover thickness on effective thermal efficiency η

5. CONCLUSIONS

This study describes a heat transfer model of a hydronically-heated bridge road (HHBR) and the validity of the hydronic bridge-road heating (HBRH) model. The critical parameters for the design of the HBRH systems and the thermal efficiency η were also examined. The effects of the thickness of the three layers making up the HHBR, the thermal conductivity, and the overburden depth of heat-carrier fluid passages on η were identified in a numerical simulation by the HBRH model.

The main conclusions drawn from the present study are as follows:

(1) The HBRH model reproduced the vertical distribution of temperatures of the HHBR found in the laboratory experiment.

(2) η diminishes exponentially with the increase in the thickness of the surface course, thermal conductivity of the deck slab and overburden depth of the hart-carrier fluid passage. On the contrary, η grows logarithmically with the increase in the thermal conductivity of the surface course and base course.

REFERENCES

1. Watanabe, H. and Fukuhara T. (1995). Heat and moisture transfer between bridge road surface and atmosphere and road freezing phenomenon, Journal of Hydroscience and Hydraulic Engineering. Vol. 39, pp. 183-188
2. Watanabe, H. and Fukuhara T. (1998). Thermal characteristics of road surface temperature in winter by thermal mapping, Journal of Snow Engineering of Japan. Vol. 14, No. 2, pp. 133-140

3. Fukuhara T., Sakai, J. and Watanabe, H. (1994). Freezing Mechanism and Estimation of Freezing on Bridge Road, Extended abstract of Fourth International Symposium on Cold Region Development in Finland, pp. 181-182
4. Zaima, T., Moriyama, K., Hayashi, T. and Tanaka, M. (1998). Non-water sprinkling snowmelt system using earth thermal for bridge road surface, Japan Society of Civil Engineers 1998 Annual Meeting. Vol. 53, pp. 494-495
5. Miyamoto, S. and Kaga, H. (1998). Study on Snow-melting and De-icing System with Dissipation Pipes on Bridge Road, Cold Region Technology Conference. Vol. 14, pp. 187-190
6. Editorial Committee on design guideline for snow melting on road. (2008). Design guideline for snow melting on road, Japan Construction Machinery and Construction Association /Hokuriku Branch. p. 158
7. Tanaka, T., Fujimoto, A. and Fukuhara, T. (2010). Dependence of thermal conductivity of drainage pavement on water content, Summaries of JSSI & JSSE Joint Conference on Snow and Ice Research - 2010/Sendai. p. 26
8. The Japan Society of Mechanical Engineers. (1993). JSME heat transfer handbook. p. 377
9. Fujimoto, A., Watanabe, H. and Fukuhara, T. (2010). Evaluation method for thermal characteristics of snow melting pavement, Japan Society of Civil Engineers 2010 Annual Meeting. Vol. 65, pp. 761-762